

AD-A198 291

FINITE-ELEMENT GRID IMPROVEMENT BY MINIMIZATION OF
STIFFNESS MATRIX TRACE(U) NATIONAL AERONAUTICS AND
SPACE ADMINISTRATION CLEVELAND OH LE.

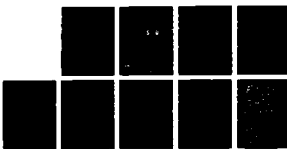
1/1

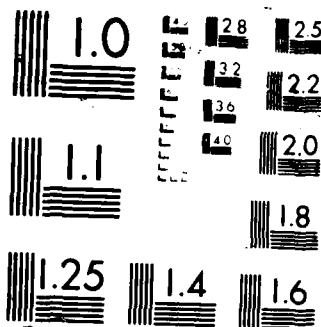
UNCLASSIFIED

M G KITTUR ET AL. DEC 87 NASA-E-3027

F/G 12/1

ML





NASA
Technical Memorandum 100255

2
DTIC FILE COPY AVSCOM
Technical Report 87-C-4

Finite-Element Grid Improvement by Minimization of Stiffness Matrix Trace

AD-A190 291

Madan G. Kittur and Ronald L. Huston
University of Cincinnati
Cincinnati, Ohio

and

Fred B. Oswald
U.S. Army Aviation Research and Technology Activity—AVSCOM
Lewis Research Center
Cleveland, Ohio

DTIC
ELECTED
S FEB 08 1988 D
CD

DISTRIBUTION STATEMENT A
Approved for public release
Distribution Unlimited

December 1987

NASA



88 2 01 112

FINITE-ELEMENT GRID IMPROVEMENT BY MINIMIZATION OF STIFFNESS MATRIX TRACE

Madan G. Kittur and Ronald L. Huston
Department of Mechanical and
Industrial Engineering
University of Cincinnati
Cincinnati, Ohio 45221-0072

and

Fred B. Oswald
National Aeronautics and Space Administration
Lewis Research Center
Cleveland, Ohio 44135-3191

SUMMARY

A new and simple method of finite-element grid improvement is presented. The objective is to improve the accuracy of the analysis. The procedure is based on a minimization of the trace of the stiffness matrix. For a broad class of problems this minimization is seen to be equivalent to minimizing the potential energy. The method is illustrated with the classical tapered bar problem examined earlier by Prager and by Masur. Identical results are obtained.

INTRODUCTION

In a general context, the finite-element method is an approximate procedure for solving differential equations. The accuracy of the method depends on (1) the number of elements, (2) the choice of interpolation functions, and (3) the location of the grid points. The number of elements, and hence the number of grid points, is usually restricted simply by computer capability and by processing costs. Also, there have been many recent advances in improving the accuracy of the finite-element method by using higher order interpolation polynomials and shape functions (*p*-method) and by exhaustive analysis with large numbers of elements (*h*-method). Some of these advances are described in the references cited herein. However, optimal grid point location (*r*-method) is far less advanced. Practical procedures for the analyst still need to be developed and refined.

One of the earliest attempts to develop a grid optimization procedure was that of Prager in 1975 (ref. 1). Prager's work provided a stimulus and a basis for later grid optimization research as recorded in references 2 to 19. Note-worthy among these efforts are the works of Shepard (refs. 11, 13, and 15), Masur (ref. 2), Turcke (refs. 8 and 9), Carroll (ref. 7), McNiece (ref. 4), Carey (ref. 16), Diaz (ref. 12), Melosh (ref. 10), Durocher (ref. 17), and their colleagues.

Prager examined a bar with a linearly varying cross section under tension. He showed that the grid producing the desired least potential energy is the one where the cross-section areas at the nodes form a geometric series. In this configuration, the strain energy is divided equally among the elements.

Masur (ref. 2) observes that this latter result of equal element strain energies is not a general characteristic of optimal meshes but instead is a result of the simple geometry of Prager's problem.

In this paper we present a finite-element grid improvement technique which is based on the minimization of the trace of the global stiffness matrix. We show that this method leads to identical results to those of Prager. It has the advantage of being simpler than traditional optimization procedures.

The method presented herein provides a mesh improvement which is based on the geometry of the body. As such, it provides a significant improvement over uniform meshes, and it produces a good first iteration for accommodating special loading configurations.

In the usual finite-element procedure, the governing equations are obtained by minimizing a functional π by varying the dependent variables of the physical problem (ref. 20). For elastostatics this is equivalent to the principle of minimum potential energy (ref. 21). This leads to the familiar system of linear algebraic equations. Attempts to minimize π with respect to the nodal coordinates, however, leads to a system of nonlinear equations. These equations are generally extremely difficult to solve even for the simplest cases. To avoid this difficulty we are proposing instead to examine the stiffness matrix to obtain information about an improvement in grid point location. Our motivation is the observation of the major role of the stiffness matrix in the value of the potential π . Also, the entries of the stiffness matrix are dependent on the grid point coordinates.

NOMENCLATURE

| | |
|-------------|---------------------------------|
| A | area |
| A_k | nodal area |
| A_2 | end area |
| A_0 | base area |
| \bar{A}_k | area of k^{th} element |
| c | area ratio (see eq. (7)) |
| E | elastic modulus |
| {f} | global force array |
| \hat{f} | transformed global force array |
| \hat{f}_i | entries of {f} |
| [K] | global stiffness matrix |
| $\hat{[K]}$ | diagonal form of $\hat{[K]}$ |

\hat{k}_i entries of $[\hat{K}]$
 L bar length
 ℓ_k length of k^{th} element
 n number of elements
 P axial load
 r_{ij} length ratio, ℓ_i/ℓ_j
 S_n sum of length ratios, $\sum_{j=1}^n r_{j1}$
 T trace of $[K]$
 $[T]$ transformation matrix
 u axial displacement
 $\{u\}$ global displacement array
 $\hat{\{u\}}$ transformed global displacement array
 \hat{u}_i entries of $\hat{\{u\}}$
 x axial coordinate
 x_k nodal coordinate
 K element stiffness matrix
 π potential energy
 ξ dimensionless axial coordinate
 ξ_k dimensionless nodal coordinate

| | | |
|----------------|------------|-------------------------------------|
| Classification | NTIS CRA&I | <input checked="" type="checkbox"/> |
| Unclassified | DOD TAB | <input type="checkbox"/> |
| Justification | | |
| By | | |
| Distribution | | |
| Availabilty | | |
| Comments | | |
| A-1 | | |

ANALYSIS

Our objective is to develop a practical and efficient procedure of grid enhancement tending towards optimization. Our thesis is that for many problems the minimization of the trace of the stiffness matrix leads to a minimization of the potential energy and, as a consequence, provides the optimal grid configuration.

To see this, consider the governing matrix equation of finite-element analysis:

$$[K]\{u\} = \{f\} \quad (1)$$

where $[K]$ is the stiffness matrix, $\{u\}$ the array of dependent variables, and $\{f\}$ the force array. We can view $[K]$ as an operator which maps $\{u\}$ into

$\{f\}$. In this context, since $[K]$ is symmetric¹ we can find an orthogonal transformation $[T]$ which diagonalizes $[K]$; that is,

$$\hat{[K]} = [T]^T [K] [T] \quad (2)$$

where $\hat{[K]}$ is a diagonal matrix. Let $[T]\{u\}$ and $[T]\{f\}$ be $\{\hat{u}\}$ and $\{\hat{f}\}$. Then the potential energy π may be expressed as

$$\pi = \frac{1}{2} \{u\}^T [K] \{u\} - \{f\}^T \{u\} = \frac{1}{2} \{\hat{u}\}^T \hat{[K]} \{\hat{u}\} - \{\hat{f}\}^T \{\hat{u}\} \quad (3)$$

In terms of the array components, π becomes

$$\pi = \sum_{i=1}^n \left(\frac{1}{2} \hat{k}_i \hat{u}_i^2 - \hat{f}_i \hat{u}_i \right) \quad (4)$$

where the \hat{k}_i ($i=1, \dots, n$) are the diagonal entries of $\hat{[K]}$.

Observe in equation (4) that the last term $- \sum_{i=1}^n \hat{f}_i \hat{u}_i$ does not explicitly involve the nodal coordinates. Therefore, $- \sum_{i=1}^n \hat{f}_i \hat{u}_i$ does not affect the minimization of π with respect to the nodal coordinates. Also, since the \hat{u}_i^2 are positive and are independent variables in the minimization of π , the minimization of π with respect to the nodal coordinates occurs when the sum of the \hat{k}_i (the trace of $\hat{[K]}$) is a minimum. Since the trace of a matrix is invariant under an orthogonal transformation, minimizing the trace of $\hat{[K]}$ is equivalent to minimizing the trace of $[K]$.

In minimizing the trace, we will not adversely affect the diagonal dominance of $[K]$ required to avoid ill-conditioning. The improved stiffness matrix we seek is the result of redistribution of the nodes and not of an arbitrary mathematical operation.

To illustrate the application of these concepts, consider the axially loaded tapered bar shown in figure 1. (This is the same problem examined by Prager (ref. 1) and Masur (ref. 2).) The objective is to determine a finite-element mesh which best predicts the axial displacement. Let the bar have length L and let it be divided into n elements with $n+1$ nodes (numbered 0 to n) as shown. Let the areas at the ends of the bar be A_0 and A_n . Let ξ be the nondimensional length parameter defined as

$$\xi = \frac{x}{L} \quad (5)$$

¹The analysis which follows is based on the symmetry of $[K]$. If $[K]$ is not symmetric, a similar analysis could be developed using nonorthogonal transformations.

Then the area at any particular ξ along the bar is

$$A = A_0(1 - c\xi) \quad (6)$$

where c is

$$c = \frac{A_0 - A_L}{A_0} \quad 0 \leq c \leq 1 \quad (7)$$

Hence, the area at the k^{th} node is

$$A_k = A_0(1 - c\xi_k) \quad (8)$$

where ξ_k is $\xi(x_k)$.

Let the individual elements have a uniform cross section. For example, let the k^{th} element have cross-section area \bar{A}_k and length ℓ_k as in figure 2. (Note that the elements do not necessarily have the same length.) Then A_k and ℓ_k are

$$\bar{A}_k = \frac{A_{k-1} + A_k}{2} \quad \left. \right\} \quad (9)$$

and

$$\ell_k = x_k - x_{k-1} = L(\xi_k - \xi_{k-1}) \quad \left. \right\}$$

The element stiffness matrix for the k^{th} element is (ref. 20)

$$[\kappa] = \frac{\bar{A}_k E}{\ell_k} \begin{bmatrix} 1 & -1 \\ -1 & 1 \end{bmatrix} \quad (10)$$

where E is the elastic modulus. Then the trace T of the global stiffness matrix is

$$T = 2E \sum_{i=1}^n \frac{\bar{A}_i}{\ell_i} = \frac{E}{L} \sum_{i=1}^n \left(\frac{A_{i-1} + A_i}{\xi_i - \xi_{i-1}} \right) \quad (11)$$

The improved node location occurs when the trace is minimized with respect to the nodal coordinates $\xi_k (k=1, \dots, n-1)$.² Hence, by setting the derivative of T with respect to ξ_k equal to zero, we obtain

²Nodes numbers 0 and n are fixed at the ends of the bar and thus not considered for optimization.

$$\frac{\partial T}{\partial \xi_k} = 0 = \frac{E}{L} \left[\frac{\frac{\partial}{\partial \xi_k} (A_{k-1} + A_k)}{\xi_k - \xi_{k-1}} + \frac{\frac{\partial}{\partial \xi_k} (A_k + A_{k+1})}{\xi_{k+1} - \xi_k} - \frac{A_{k-1} + A_k}{(\xi_k - \xi_{k-1})^2} + \frac{A_k + A_{k+1}}{(\xi_{k+1} - \xi_k)^2} \right] \quad (12)$$

Using equation (9) and simplifying we obtain

$$A_{k+1} = A_k \left[\left(\frac{\ell_{k+1}}{\ell_k} \right)^2 - 1 \right] + A_{k-1} \left(\frac{\ell_{k+1}}{\ell_k} \right)^2 + c A_0 \left(\frac{\ell_{k+1}}{L} \right) \left[\left(\frac{\ell_{k+1}}{\ell_k} \right) + 1 \right] \quad (13)$$

To simplify the analysis it is convenient to introduce the length ratio parameter r_{ij} defined as ℓ_i/ℓ_j . Then the ratio ℓ_{k+1}/ℓ_k may be written as

$$\frac{\ell_{k+1}}{\ell_k} = \frac{\frac{\ell_{k+1}}{\ell_1}}{\frac{\ell_k}{\ell_1}} = \frac{r_{k+1,1}}{r_{k1}} \quad (14)$$

Then L/ℓ_k is

$$\frac{L}{\ell_k} = \sum_{j=1}^n \frac{\ell_j}{\ell_k} = \sum_{j=1}^n \frac{r_{j1}}{r_{k1}} = \frac{s_n}{r_{k1}} \quad (15)$$

where s_n is defined as $\sum_{j=1}^n r_{j1}$. Using this notation, we can rewrite equation (13) as

$$A_{k+1} = A_k \left[\left(\frac{r_{k+1,1}}{r_{k1}} \right)^2 - 1 \right] + A_{k-1} \left(\frac{r_{k+1,1}}{r_{k1}} \right)^2 + \frac{c A_0 r_{k+1,1}}{s_n} \left[\left(\frac{r_{k+1,1}}{r_{k1}} \right) + 1 \right] \quad (16)$$

Also, ξ_k may be written as

$$\xi_k = \frac{\ell_1 + \ell_2 + \dots + \ell_k}{L} = \frac{1 + r_{21} + r_{31} + \dots + r_{k1}}{s_n} = \frac{1}{s_n} \sum_{j=1}^n r_{j1} = \frac{s_k}{s_n} \quad (17)$$

Then, from equation (8), A_k may be written as

$$A_k = A_0 \left[1 - c \left(\frac{S_k}{S_n} \right) \right] \quad (18)$$

Specifically, A_1 and A_2 are

$$\left. \begin{aligned} A_1 &= A_0 \left[1 - \left(\frac{c}{S_n} \right) \right] \\ A_2 &= A_0 \left[1 - c \frac{(1 + r_{21})}{S_n} \right] \end{aligned} \right\} \quad (19)$$

and

To obtain the element area ratios let $k = 1$ in equation (16). A_2 is then

$$A_2 = A_1 \left(r_{21}^2 - 1 \right) + A_0 r_{21}^2 + c A_0 r_{21} \frac{r_{21} + 1}{S_n} \quad (20)$$

Then, by using equations (19) to eliminate A_1 and A_2 , we obtain

$$S_n (1 - r_{21}) = c \quad (21)$$

From the first of equations (19) we have

$$\left. \begin{aligned} A_1 &= A_0 r_{21} \\ \frac{A_1}{A_0} &= r_{21} \end{aligned} \right\} \quad (22)$$

or

Similarly, the second of equations (19) leads to

$$\left. \begin{aligned} A_2 &= A_0 r_{21}^2 \\ \frac{A_2}{A_1} &= r_{21} \end{aligned} \right\} \quad (23)$$

or

Next, let $k = 2$ in equation (16). By using the same procedure we obtain

$$1 - r_{32} = \frac{c}{S_n} (1 - r_{32} + r_{21}) \quad (24)$$

But, in view of equation (21) this becomes

$$\left. \begin{aligned} 1 - r_{32} &= (1 - r_{21})(1 - r_{32} + r_{21}) \\ r_{21}(r_{32} - r_{21}) &= 0 \end{aligned} \right\} \quad (25)$$

or

Thus,

$$r_{32} = r_{21} \quad (26)$$

From equation (18) we have

$$A_3 = A_0 \left[1 - c \left(\frac{S_3}{S_n} \right) \right] = A_0 r_{21}^3 \quad (27)$$

Therefore, we obtain

$$\frac{A_3}{A_2} = \frac{A_2}{A_1} = \frac{A_1}{A_0} = r_{21} = r_{32} \quad (28)$$

Proceeding similarly for $k = 3, 4, \dots$, we obtain

$$\frac{A_n}{A_{n-1}} = \frac{A_{n-1}}{A_{n-2}} = \dots = \frac{A_1}{A_0} = r_{21} = r_{32} = \dots = r_{n,n-1} \quad (29)$$

Thus, we have the relations

$$\left. \begin{aligned} r_{31} &= r_{21} r_{32} = r_{21}^2 \\ r_{41} &= r_{43} r_{32} r_{21} = r_{21}^3, \dots, r_{k1} = r_{21}^{k-1} \end{aligned} \right\} \quad (30)$$

Hence, S_k is the geometric series

$$S_k = 1 + r_{21} + r_{21}^2 + \dots + r_{21}^{k-1} = \frac{1 - r_{21}^k}{(1 - r_{21})} \quad (31)$$

Then, from equations (18) and (21), we have

$$\left. \begin{aligned} A_k &= A_0 [1 - (1 - r_{21}^k)] = A_0 r_{21}^k \\ A_n &= A_0 r_{21} = A_0 \end{aligned} \right\} \quad (32)$$

and then

$$A_n = A_0 r_{21} = A_0$$

Then, from equation (7) we see that r_{21} is

$$r_{21} = (1 - c)^{1/n} \quad (33)$$

Finally, by substituting into equation (17) we have

$$\begin{aligned} \xi_k &= \frac{l_1}{L} (1 + r_{21} + r_{31} + \dots + r_{k1}) = (1 - r_{21}) \frac{1 + r_{21} + r_{21}^2 + \dots + r_{21}^{k-1}}{c} \\ &= \frac{1 - r_{21}^k}{c} = \frac{1 - (1 - c)^{k/n}}{c} \end{aligned} \quad (34)$$

This is the result obtained by Prager (ref. 1) in his analysis of the same problem.

DISCUSSION

First, observe that in equation (34) for a uniform thickness beam $c = 0$ and thus ξ_k is undetermined. This means that for a uniform thickness beam the nodal positions are arbitrary; that is, all meshes are equally optimal for a uniform thickness beam.

Next, consider again the element stiffness matrix of equation (10). From equations (8) and (34) the scalar multiplier is

$$\frac{\bar{E}A_k}{l_k} = \frac{E(A_{k-1} + A_k)}{2L(\xi_k - \xi_{k-1})} = \frac{A_0 c}{2L} \left(\frac{1 + r_{21}}{1 - r_{21}} \right) \quad (35)$$

Since this is a constant (independent of k) the element stiffness matrix is the same for each element. This means that each element has the same strain energy. Masur (ref. 2) has suggested that this result is due to the simple geometry of the problem.

Even with this simple geometry, however, the analysis needed to determine the optimal nodal positions has been extremely detailed. With more complex geometries the analysis will become intractable. Alternatively, a more convenient method of improving the nodal positions is to examine the trace of the stiffness matrix and to adjust the nodal positions to minimize the trace. The criteria for minimizing the trace of the stiffness matrix is a comparatively

simple procedure - readily amenable to the development of computer algorithms for optimal nodal locations.

In the preceding discussion, we have ignored any consideration of the effects of concentrated loads or boundary/edge effects. It is common engineering practice to use a fine (dense) grid in highly loaded regions and to place a grid point specifically at the point of application of a concentrated load. The trace minimization suggested here is intended to aid in the discretization process at locations removed from concentrated loads. Our justification is based on Saint-Venant's principle that localized effects disappear at short distances.

A principal question with the minimum trace method is: What is the range of applicability? The authors have found the method to lead to significant decreases in potential energy from that of a uniform mesh for structural and heat-transfer problems. The range of applicability is currently being explored. Numerical algorithms using this procedure are being developed. Finally, the influence of values of second and higher invariants of the stiffness matrix needs to be explored.

NUMERICAL EXAMPLE

To illustrate the value of optimizing the mesh, consider an axially loaded bar which tapers to 1/3 the base area as in figure 3. Specifically, let P , A_0 , c , E , and L have the following values:

$$P = 20 \text{ N}$$

$$A_0 = 0.0015 \text{ m}^2$$

$$c = \frac{2}{3}$$

$$E = 2.07 \times 10^{11} \text{ N/m}^2$$

$$L = 4 \text{ m}$$

The objective is to find the axial displacement.

From elementary mechanics the axial displacement u at any location x is

$$u = -\frac{PL}{A_0 Ec} \ln\left(1 - \frac{cx}{L}\right) \quad (37)$$

To compare the displacement results of finite-element models with equation (37), four models of the bar, each having four elements, were examined. One of the models had a uniform nodal distribution. Another had the "optimal" mesh as developed in equation (34). The remaining two models had arbitrarily selected nodal distributions. The nodal displacements were evaluated using the four model's and compared with the displacement calculated by equation (37). Table I shows the results. Table II presents an error analysis and also an

L_2 -norm of the error. As expected, the optimum mesh produces the least L_2 error.

CONCLUSIONS

A new method of finite-element grid improvement based on the principle of minimization of the trace of the stiffness matrix was developed. This procedure is equivalent to minimizing the potential energy of the model by dividing the strain energy equally among the elements. The following conclusions are made:

1. The analysis and the numerical results demonstrate the potential usefulness of the trace minimization mesh improvement method.
2. Minimization of the trace of the stiffness matrix is a relatively simple mesh optimization procedure. It is readily adaptable to algorithm development.
3. Trace minimization can be used in combination with other grid optimization techniques. Indeed, it can provide a starting mesh for iteration techniques, useful for specialized loading.
4. The principal benefit of the trace minimization method is accuracy of analysis as opposed to efficiency of analysis.

REFERENCES

1. Prager, W.: A Note on the Optimal Choice of Finite Element Grids. *Comput. Methods Appl. Mech. Eng.*, vol. 6, no. 3, Nov. 1975, pp. 363-366.
2. Masur, E.F.: Some Remarks on the Optimal Choice of Finite Element Grids. *Comput. Methods Appl. Mech. Eng.*, vol. 14, May 1978, pp. 237-248.
3. Tang, J.W. and Turcke, D.J.: Characteristics of the Optimal Grids. *Comput. Methods Appl. Mech. Eng.*, vol. 11, no. 1, Apr. 1977, pp. 31-37.
4. McNeice, G.M. and Marcal, P.V.: Optimization of Finite Element Grids Based on Minimum Potential Energy. *J. Eng. Ind.*, vol. 95, no. 1, Feb. 1973, pp. 186-190.
5. Carroll, W.E.: Inclusive Criteria for Optimum Grid Generation in the Discrete Analysis Technique. *Comput. Struct.*, vol. 6, no. 4-5, Aug.-Oct. 1976, pp. 333-337.
6. Pederson, P.: Some Properties of Linear Strain Triangles and Optimal Finite Element Models. *Int. J. Numer. Methods Eng.*, vol. 7, no. 4, 1973, pp. 415-431.
7. Carroll, W.E. and Barker, R.M.: A Theorem for Optimum Finite Element Idealizations. *Int. J. Solids Struct.*, vol. 9, no. 7, July 1973, pp. 883-895.

8. Turcke, D.J. and McNeice, G.M.: Guidelines for Selecting Finite Element Grids Based on an Optimization Study. *Comput. Struct.*, vol. 4, no. 3, May 1974, pp. 499-519.
9. Turcke, D.: On Optimum Finite Element Grid Configurations. *AIAA J.*, vol. 14, no. 2, Feb. 1976, pp. 264-265.
10. Melosh, R.J. and Marcal, P.V.: An Energy Basis for Mesh Refinement of Structural Continua. *Int. J. Numer. Methods Eng.*, vol. 11, no. 7, 1977, pp. 1083-1092.
11. Shephard, M.S.: Finite Element Grid Optimizatiion - A Review. *Finite Element Grid Optimization*, M.S. Shepard and R.H. Gallagher, eds., ASME, 1979, pp. 1-13.
12. Diaz, A.R., et al.: Design of an Optimal Grid for Finite Element Methods. *J. Struct. Mech.*, vol. 11, no. 2, 1983, pp. 215-230.
13. Shephard, M.S.; Gallagher, R.H.; and Abel, J.F.: The Synthesis of Near-Optimum Finite Element Meshes with Interactive Computer Graphics. *Int. J. Numer. Methods Eng.*, vol. 15, no. 7, 1980, pp. 1021-1039.
14. Babuska, I. and Rheinboldt, W.C.: A-Posteriori Error Estimates for the Finite Element Method. *Int. J. Numer. Methods Eng.*, vol. 12, no. 10, 1978, pp. 1597-1615.
15. Shephard, M.S.: An Algorithm for Defining a Single Near-Optimum Mesh for Multiple-Load-Case Problems. *Int. J. Numer. Methods Eng.*, vol. 15, no. 4, 1980, pp. 617-625.
16. Carey, G.F.: A Mesh-Refinement Scheme for Finite Element Computations. *Comput. Methods Appl. Mech. Eng.*, vol. 7, no. 1, Jan. 1976, pp. 93-105.
17. Durocher, L.L. and Stango, R.J.: Finite Element Mesh Optimization and Enrichment Techniques. *Struc. Mech. Software Series*, Vol. III, N. Perrone, W. Pilkey, and B. Pilkey, eds., University Press of Virginia, 1980, pp. 245-262.
18. Hirai, I.; Wang, B.P.; and Pilkey, W.D.: An Efficient Zooming Method for Finite Element Analysis. *Int. J. Numer. Methods Eng.*, vol. 20, no. 9, Sept. 1984, pp. 1671-1683.
19. Hirai, I., et al.: An Exact Zooming Method. *Finite Elements Anal. Des.*, vol. 1, no. 1, Apr. 1985, pp. 61-69.
20. Huston, R.L. and Passerello, C.E.: Finite Element Methods - An Introduction. Marcel Dekker, 1984, pp. 28, 151.
21. Sokolnikoff, I.S.: Mathematical Theory of Elasticity. R.E. Krieger Publishing, Malabar, FL, 1983, p. 385.

TABLE I. - COMPARISON OF AXIAL DISPLACEMENTS FOR THE BAR OF FIGURE 3 CALCULATED USING VARIOUS MODELS

| Axial location, x , m | Exact displacement (eq. (37)), 10^{-9} m | Displacements computed using various models, 10^{-9} m | | | |
|-------------------------------|--|---|----------------------------|----------|----------|
| | | Uniform mesh | "Optimum" mesh (Prager) | Mesh 3 | Mesh 4 |
| 0.0 | 0.0 | 0.0 | 0.0 | 0.0 | 0.0 |
| .5 | 33.6276 | ----- | ----- | 33.60639 | 33.60639 |
| 1.0 | 70.46244 | 70.2679 | ----- | 70.41338 | ----- |
| 1.4409860 | 106.1461 | ----- | 105.482 | ----- | ----- |
| 2.0 | 156.702 | 156.1509 | ----- | 206.8158 | 15.56506 |
| 2.5 | 208.3078 | ----- | 210.9648 | ----- | 207.1804 |
| 2.5358986 | 212.2923 | ----- | ----- | ----- | ----- |
| 3.0 | 267.883 | 266.5719 | ----- | ----- | ----- |
| 3.3678522 | 318.4384 | ----- | 316.4529 | ----- | ----- |
| 4.0 | 424.5845 | 421.1612 | 421.940 | 417.6195 | 417.9814 |

TABLE II. - ERROR ANALYSIS

| Axial location, x , m | Error for various meshes, 10^{-9} m | | | |
|-------------------------------|--|----------------------------|-----------|----------|
| | Uniform mesh | "Optimum" mesh (Prager) | Mesh 3 | Mesh 4 |
| 0.0 | 0.0 | 0.0 | 0.0 | 0.0 |
| .5 | ----- | ----- | .02121 | .02121 |
| 1.0 | .1945411 | ----- | .04906 | ----- |
| 1.441 | ----- | .664118 | ----- | ----- |
| 2.0 | .5506105 | ----- | ----- | 1.0514 |
| 2.5 | ----- | ----- | 1.492 | 1.1274 |
| 2.536 | ----- | 1.32769 | ----- | ----- |
| 3.0 | 1.311108 | ----- | ----- | ----- |
| 3.368 | ----- | 1.985439 | ----- | ----- |
| 4.0 | 3.423228 | 2.64433 | 6.965 | 6.6031 |
| L_2 -Norm | 3.7119418 | 3.6246009 | 7.1232118 | 6.780697 |

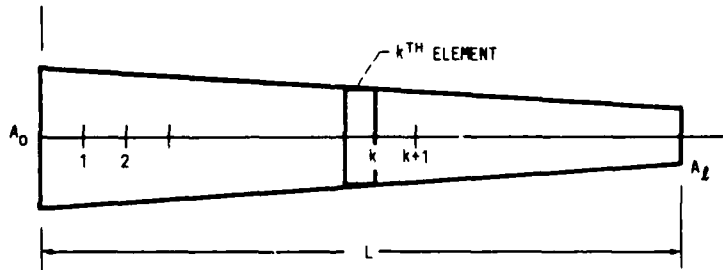


FIGURE 1. - LINEAR TAPERED BAR.

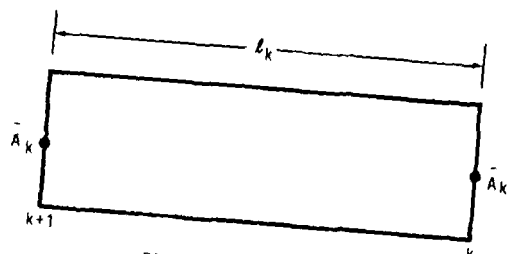


FIGURE 2. - k^{TH} ELEMENT.

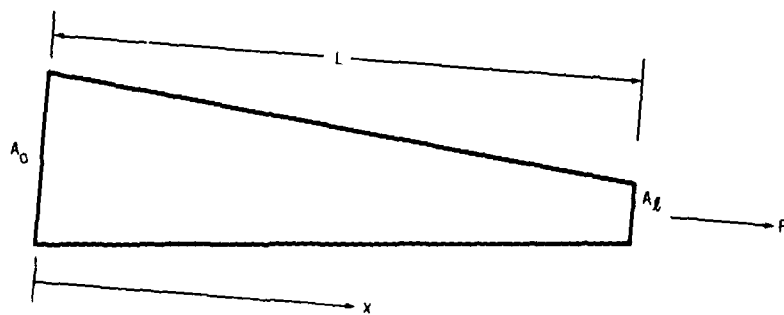


FIGURE 3. - EXAMPLE BAR AND LOADING.



National Aeronautics and
Space Administration

Report Documentation Page

| | | | | |
|---|--|-----------------|-----------------------------|----------------------------|
| 1. Report No | NASA TM-100255 AVSCOM TM-87-C-4 | | 2. Government Accession No. | 3. Recipient's Catalog No. |
| 4. Title and Subtitle | Finite-Element Grid Improvement by Minimization of Stiffness Matrix Trace | | | |
| 5. Report Date | December 1987 | | | |
| 6. Performing Organization Code | | | | |
| 7. Author(s) | Madan G. Kittur, Ronald L. Huston, and Fred B. Oswald | | | |
| 8. Performing Organization Report No | E-3827 | | | |
| 9. Performing Organization Name and Address | NASA Lewis Research Center Cleveland, Ohio 44135-3191 and Propulsion Directorate U.S. Army Aviation Research and Technology Activity—AVSCOM Cleveland, Ohio 44135-3191 | | | |
| 10. Work Unit No. | 505-63-51 | | | |
| 11. Contract or Grant No. | | | | |
| 12. Sponsoring Agency Name and Address | National Aeronautics and Space Administration Washington, D.C. 20546-0001 and U.S. Army Aviation Systems Command St. Louis, Mo. 63120-1798 | | | |
| 13. Type of Report and Period Covered | Technical Memorandum | | | |
| 14. Sponsoring Agency Code | | | | |
| 15. Supplementary Notes | Madan G. Kittur and Ronald L. Huston, University of Cincinnati, Dept. of Mechanical and Industrial Engineering, Cincinnati, Ohio 45221; Fred B. Oswald, NASA Lewis Research Center. | | | |
| 16. Abstract | A new and simple method of finite-element grid improvement is presented. The objective is to improve the accuracy of the analysis. The procedure is based on a minimization of the trace of the stiffness matrix. For a broad class of problems this minimization is seen to be equivalent to minimizing the potential energy. The method is illustrated with the classical tapered bar problem examined earlier by Prager and by Masur. Identical results are obtained. | | | |
| 17. Key Words (Suggested by Author(s)) | Finite element Mesh Grid optimization Transmissions | | | |
| 18. Distribution Statement | Unclassified - Unlimited Subject Category 37 | | | |
| 19. Security Classif. (of this report) | 20. Security Classif. (of this page) | 21. No of pages | 22. Price | |
| Unclassified | Unclassified | 15 | A02 | |

END

DATE

FI/MED

4-88

DTIC